天 氣 學 二

(Synoptic Meteorology II)

上課時間: 10:20～12:10 Wednesday, B105

授課教師: 游政谷

email: yuku@ntu.edu.tw

Chapter 3 Tropical Cyclones

3.2 Structure of mature TCs

Streamlines of Hurricane Inez (1966)

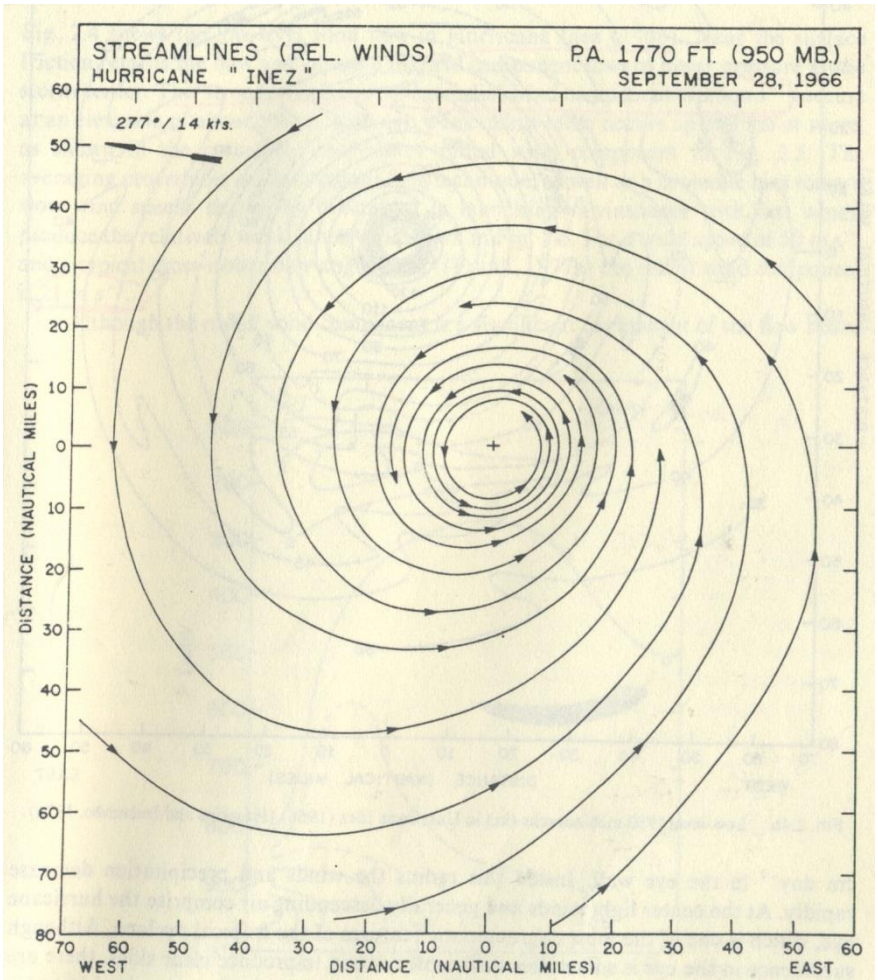

FIG. 2.4a. Low-level (950 mb) streamlines in Hurricane Inez (1966) (Hawkins and Imbembo, 1976).

Isotachs (kt) of Inez (1966)

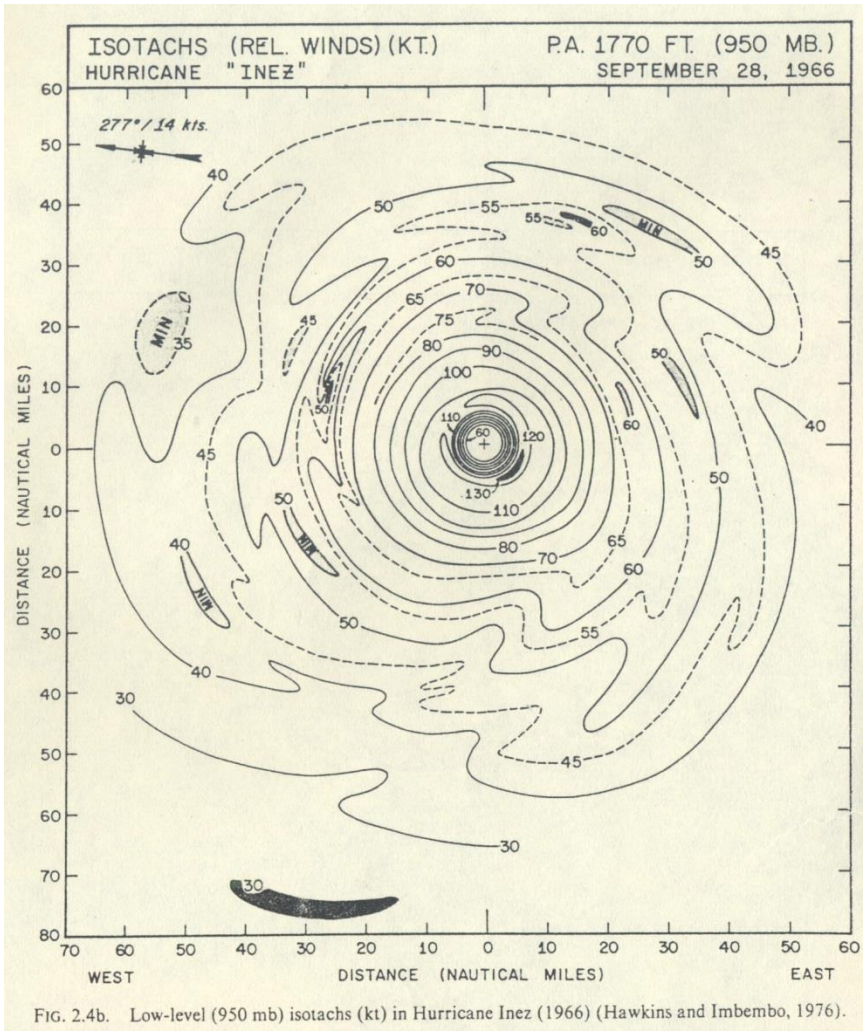

FIG. 2.4b. Low-level (950 mb) isotachs (kt) in Hurricane Inez (1966) (Hawkins and Imbembo, 1976).

It is helpful to use cylindrical coordinates (r, θ, z) to describe the structure and dynamics of the tropical cyclone system (a set of equations to be illustrated in the class)

Radial-distance-height cross section, as calculated by

$$F(r,z) = \frac{1}{2\pi}\int_0^{2\pi} F(r,\theta,z)d\theta$$

is usually used to depict axisymmetric structure of tropical cyclones

Schematic illustrating the secondary circulation of a mature hurricane

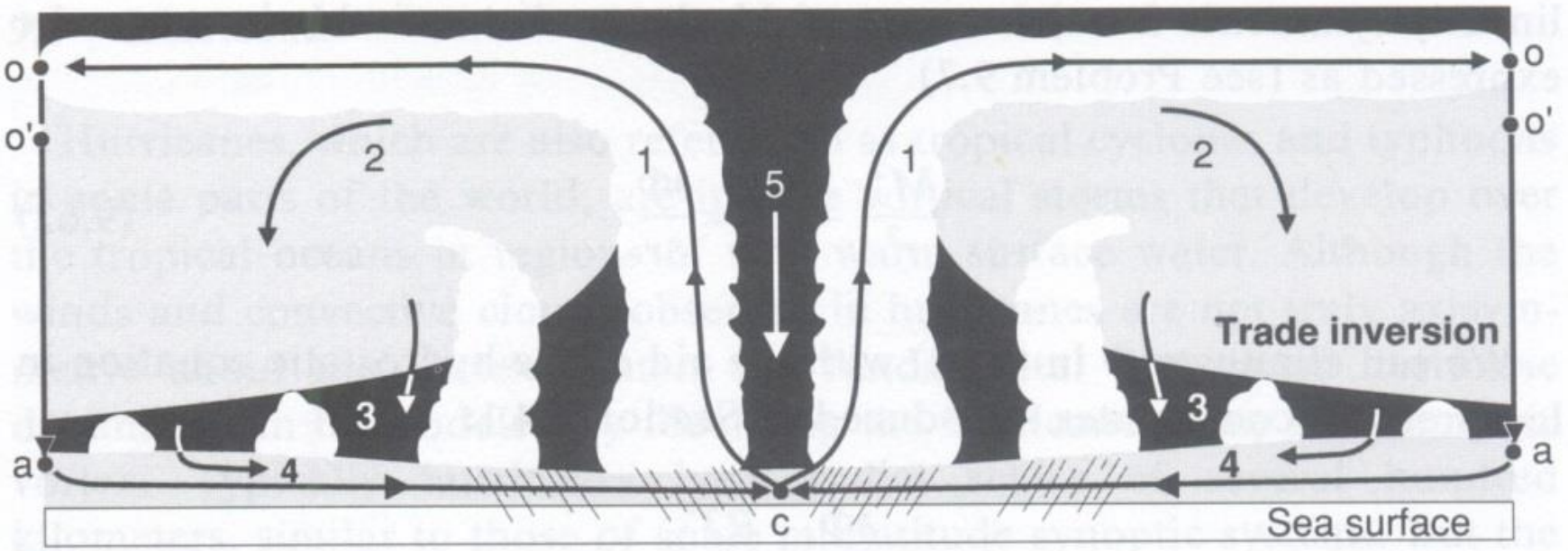

Schematic cross section of the secondary meridional circulation in a mature hurricane. Air spirals in toward the eye (region 5) in the boundary layer (region 4), ascends along constant-M surfaces in the eyewall cloud (region 1), and slowly subsides and dries in regions 2 and 3. (After Emanuel, 1988.)

mean radial wind

mean tangential wind

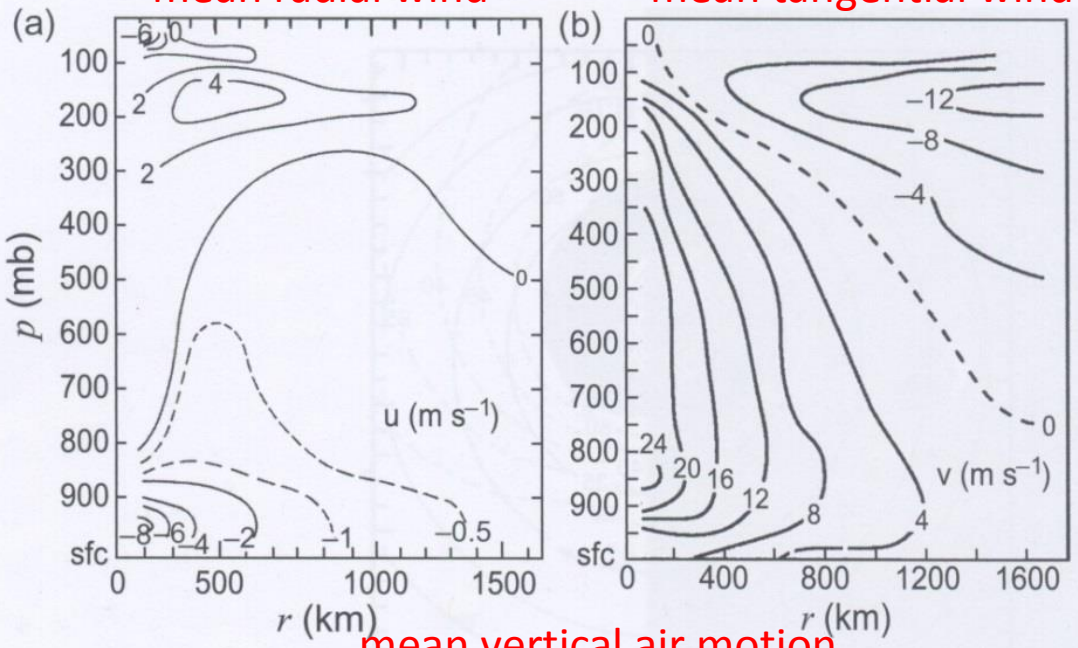

mean vertical air motion

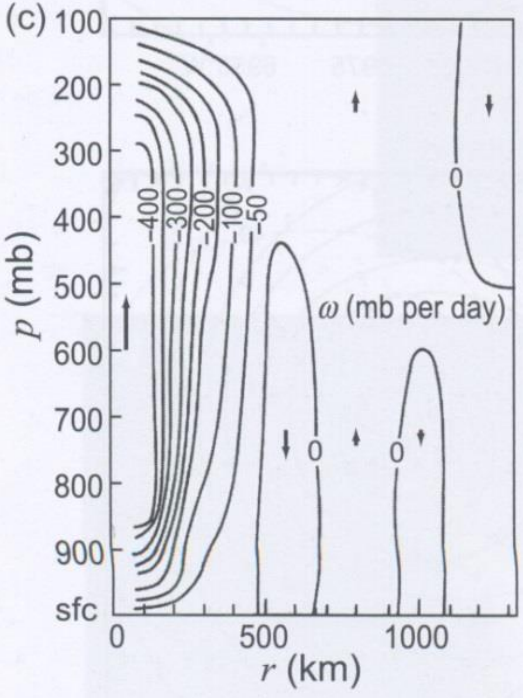

Temperature anomaly for Hurricane Inez (1966)

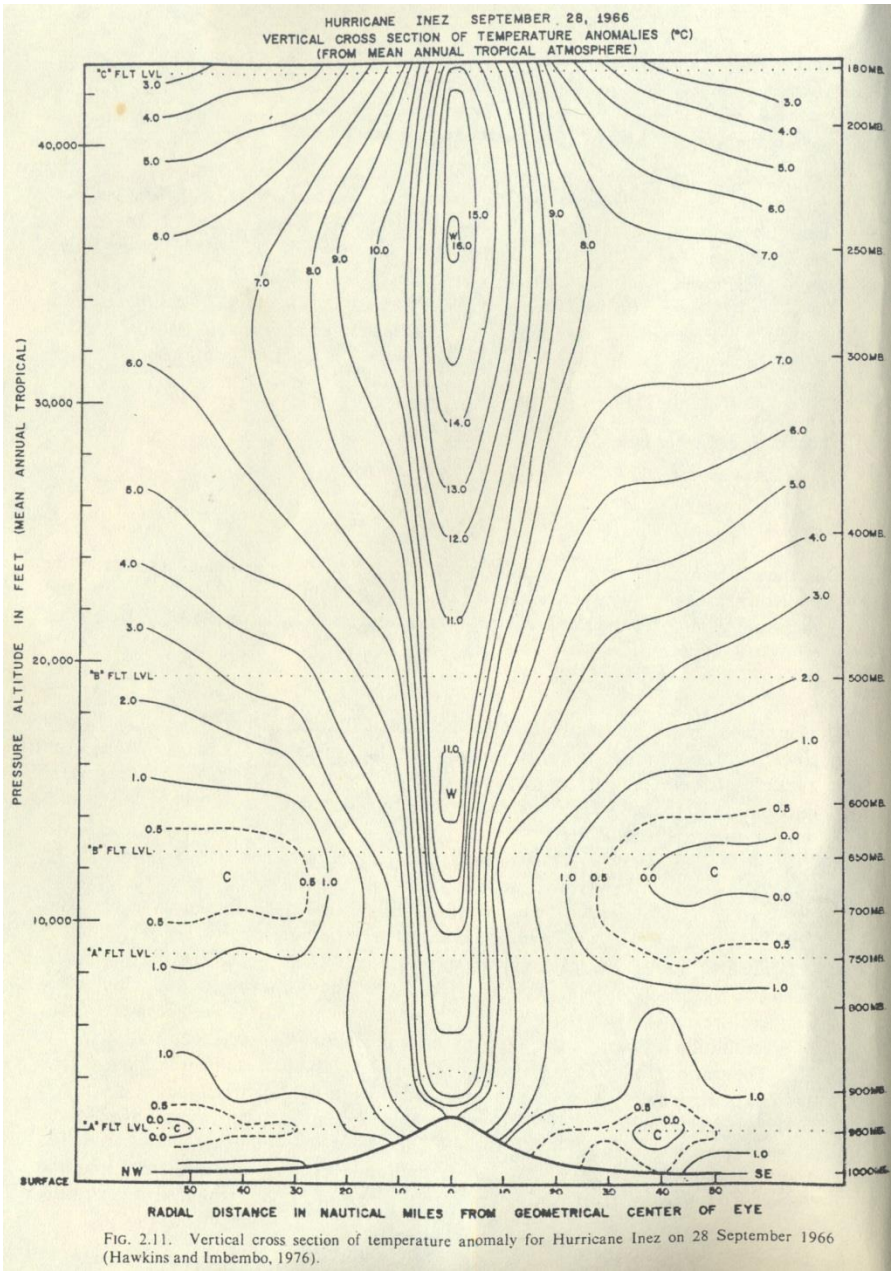

FIG. 2.11. Vertical cross section of temperature anomaly for Hurricane Inez on 28 September 1966 (Hawkins and Imbembo, 1976).

Aircraft observed tangential wind speed and D values in Hurricane Anita (1977)

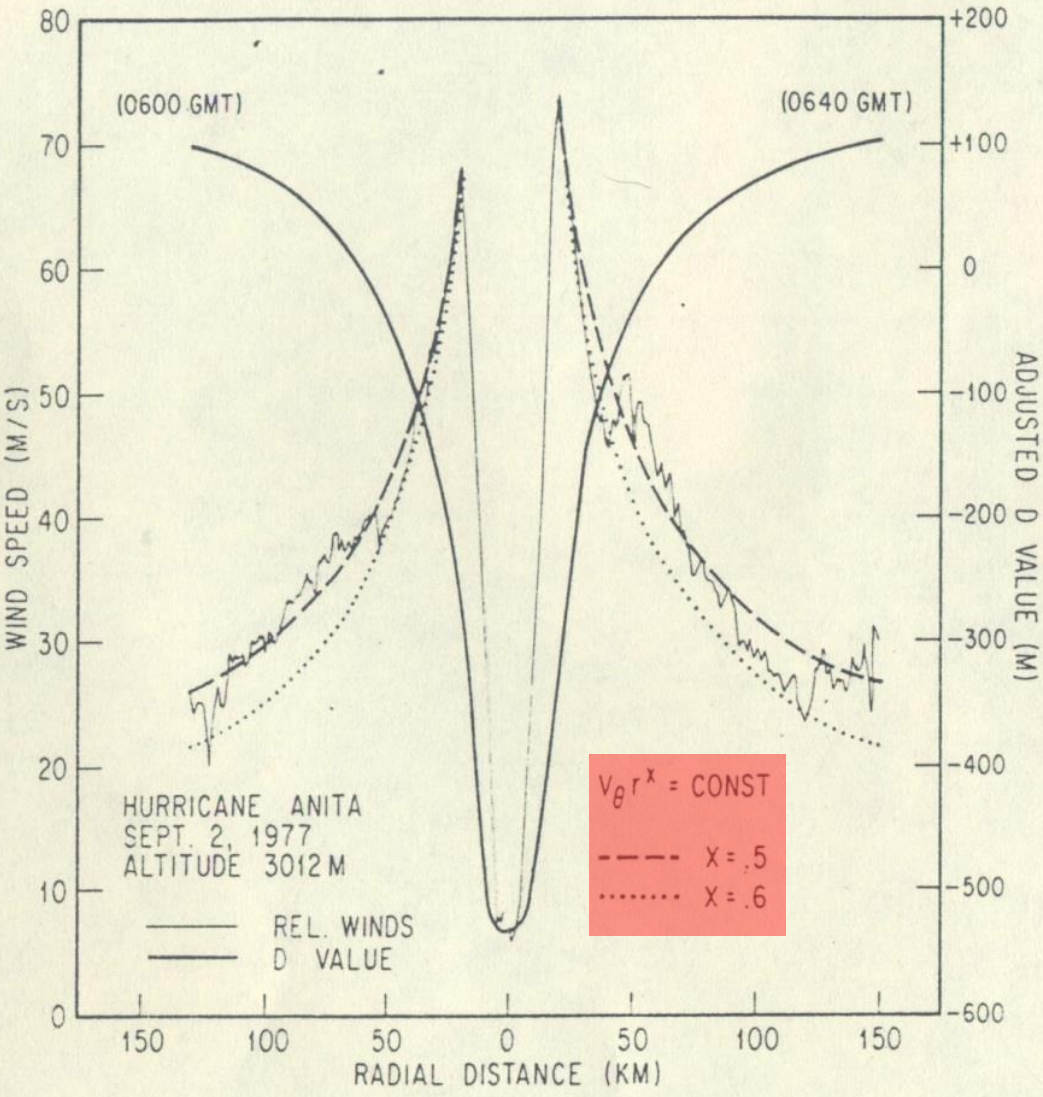

FIG. 2.8. Radial profiles of tangential wind speed (m s^{-1}) and D values (departure of isobaric height from reference value) in Hurricane Anita. Also shown are graphs $V_\theta r^x$ = constant for values of x = 0.5 and 0.6. (Sheets, 1980).

Cloud and precipitation of mature TCs

View from satellite images

Hurricane Katrina (2005)

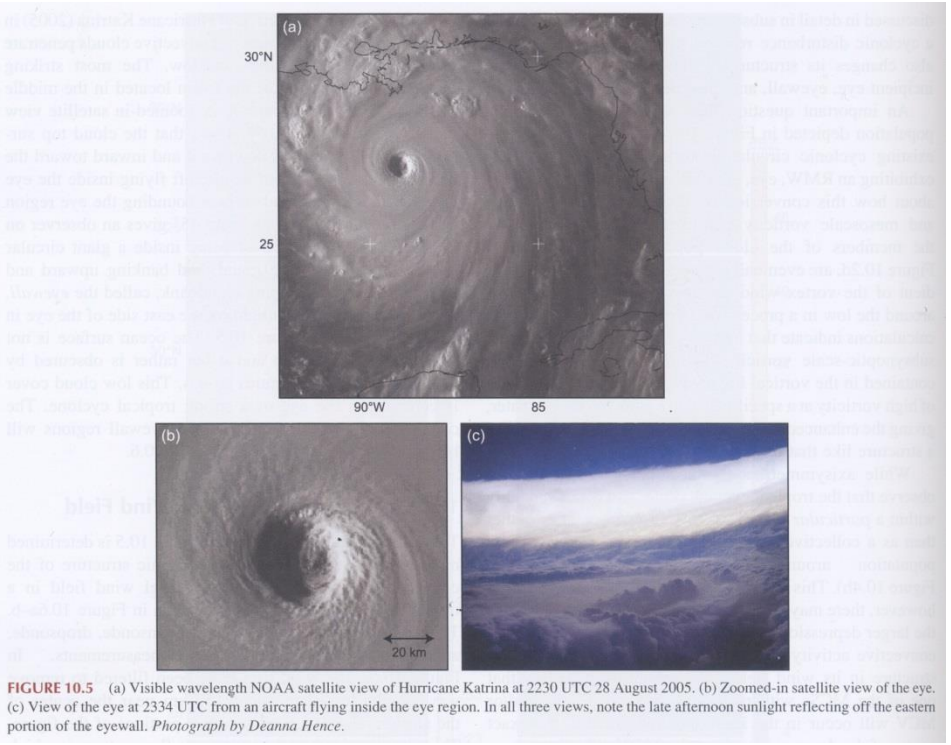

FIGURE 10.5 (a) Visible wavelength NOAA satellite view of Hurricane Katrina at 2230 UTC 28 August 2005. (b) Zoomed-in satellite view of the eye. (c) View of the eye at 2334 UTC from an aircraft flying inside the eye region. In all three views, note the late afternoon sunlight reflecting off the eastern portion of the eyewall. *Photograph by Deanna Hence.*

Schematic illustrating different types of rainbands within tropical cyclones

- Eyewall
- Secondary rainbands
- Principal rainband
- Distant rainbands

(or outer rainbands)

Tropical cyclone Rainbands (TCRs)

颱風雨帶

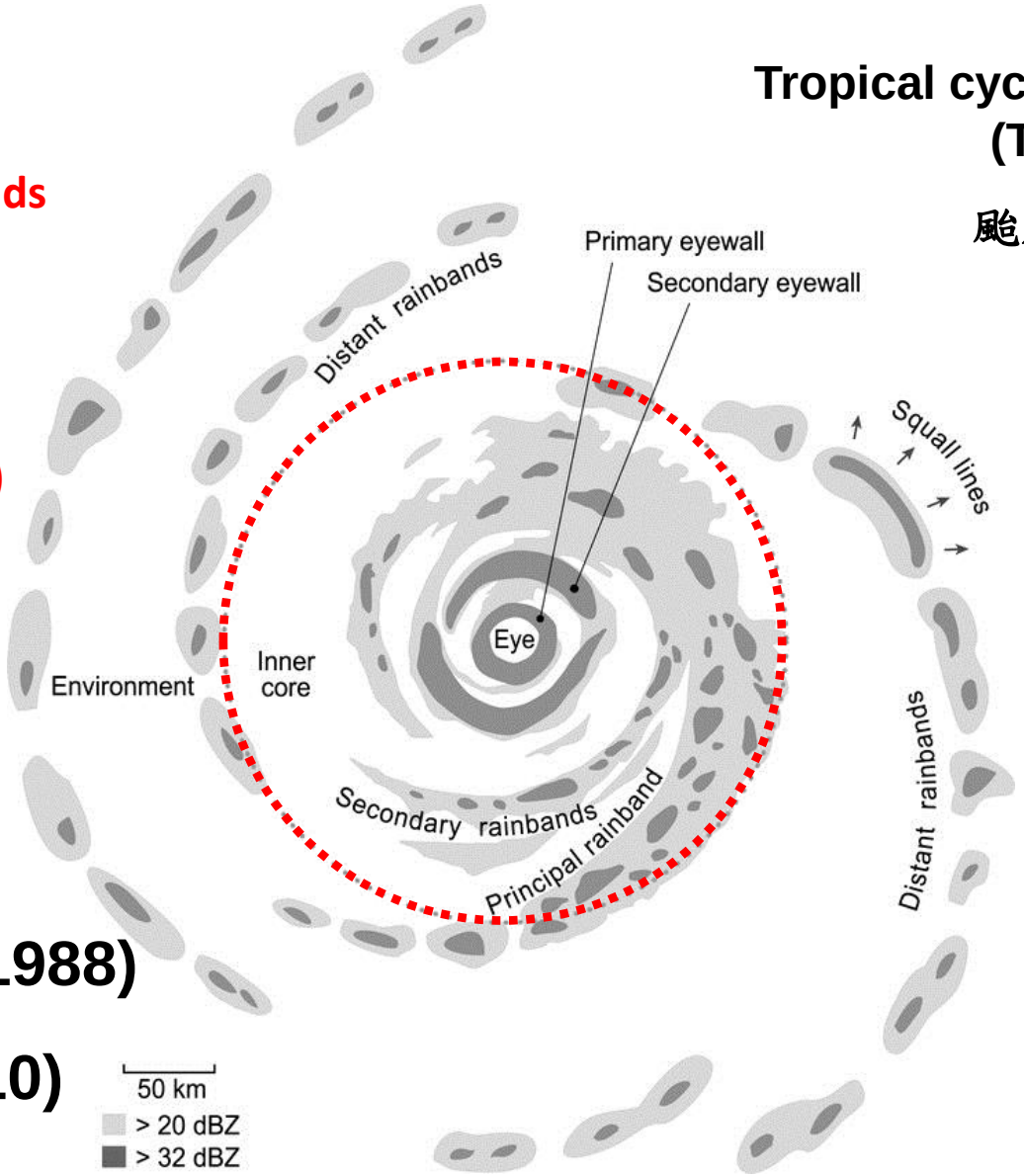

Willoughby (1988)

Houze (2010)

View from radar images

Sinlaku (2008)

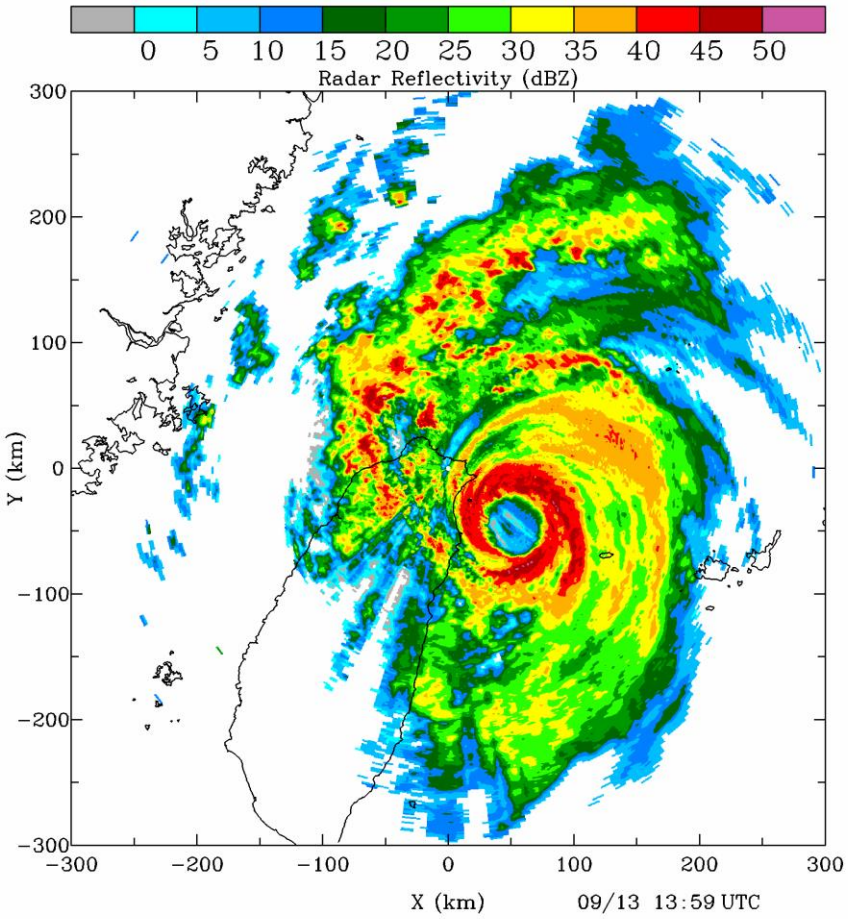

Nari (2001)

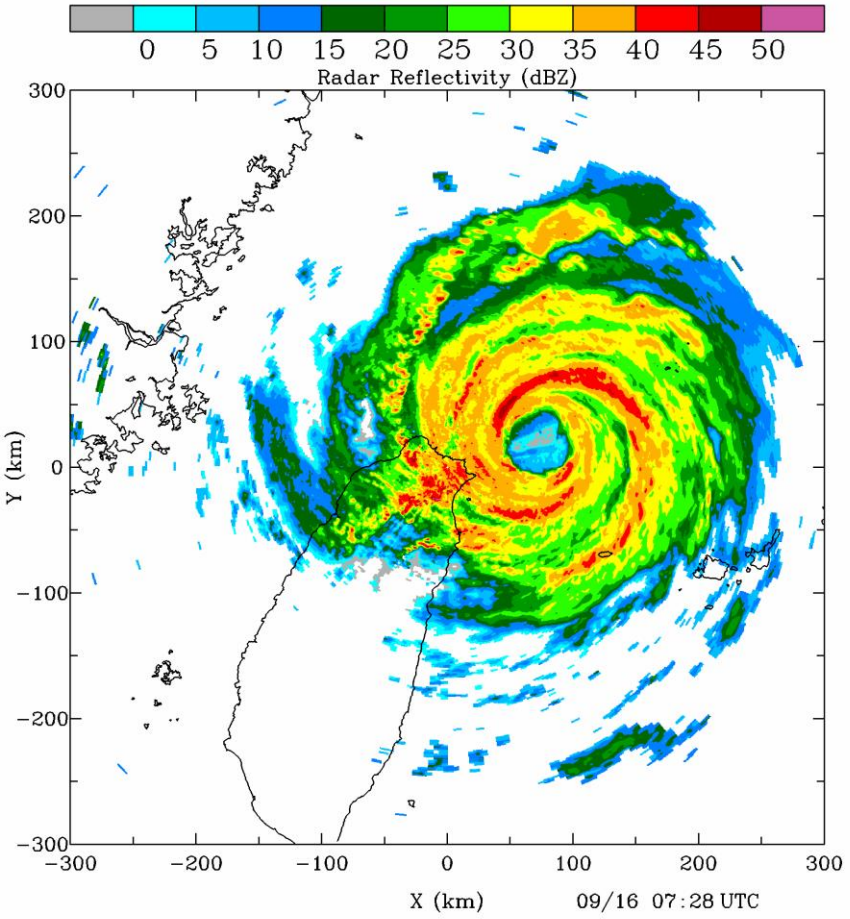

Schematic illustrating the radius-height circulation of the inner core of Hurricane Alicia (1983)

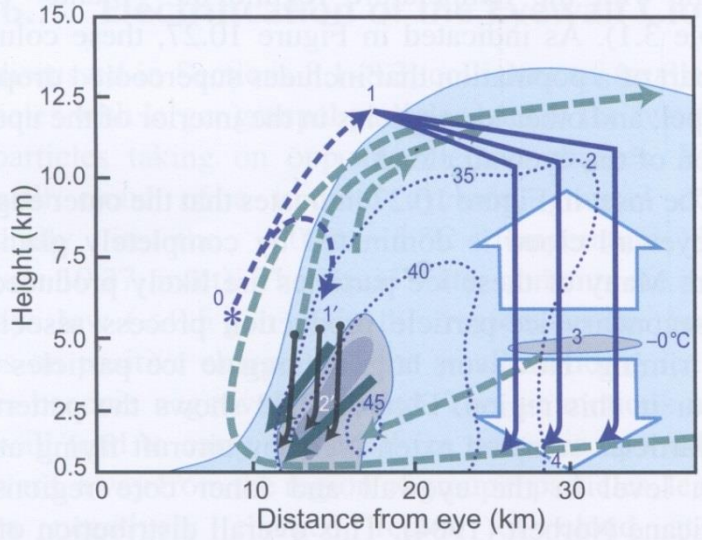

FIGURE 10.25 Schematic of the radius–height circulation of the inner core region of Hurricane Alicia (1983), as observed by airborne dual-Doppler radar. Shading depicts the reflectivity field, with contours at 5, 30, and 35 dBZ. The primary (tangential) circulation ($\bar{v}$ in m s^{-1}) is depicted by dotted lines and the secondary circulation by the wide dashed streamlines. The convective downdrafts are denoted by the thick solid arrows, while mesoscale up- and downdrafts are shown by the broad arrows. Thin dashed and solid trajectories denote paths followed by hydrometeors emanating from the location of the asterisk. Numbers along the trajectories identify points corresponding to horizontal locations in Figure 10.26. *From Marks and Houze (1987). Republished with permission of the American Meteorological Society.*

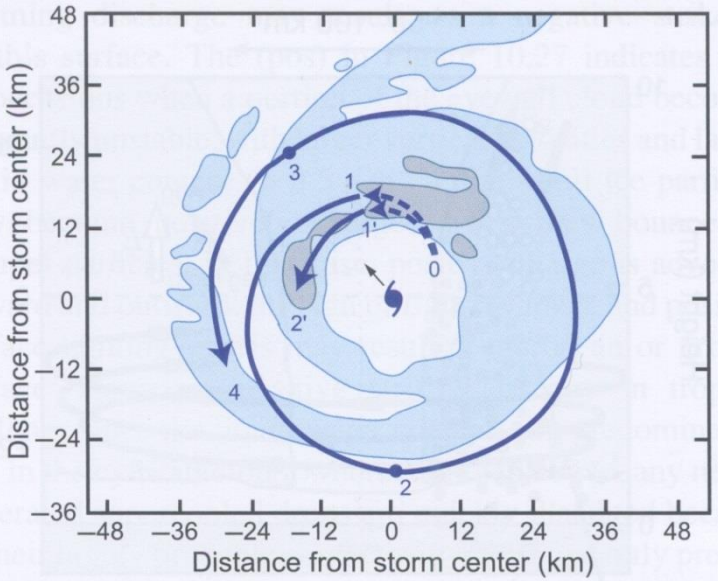

FIGURE 10.26 Horizontal projections of the paths of precipitation particle trajectories superimposed on the radar-echo pattern of Hurricane Alicia (1983). The echo contours are for 20 and 35 dBZ. The numbers show how the trajectories correspond to the vertical cross section in Figure 10.25. *From Marks and Houze (1987). Republished with permission of the American Meteorological Society.*

Airflow and precipitation structures of TCRs

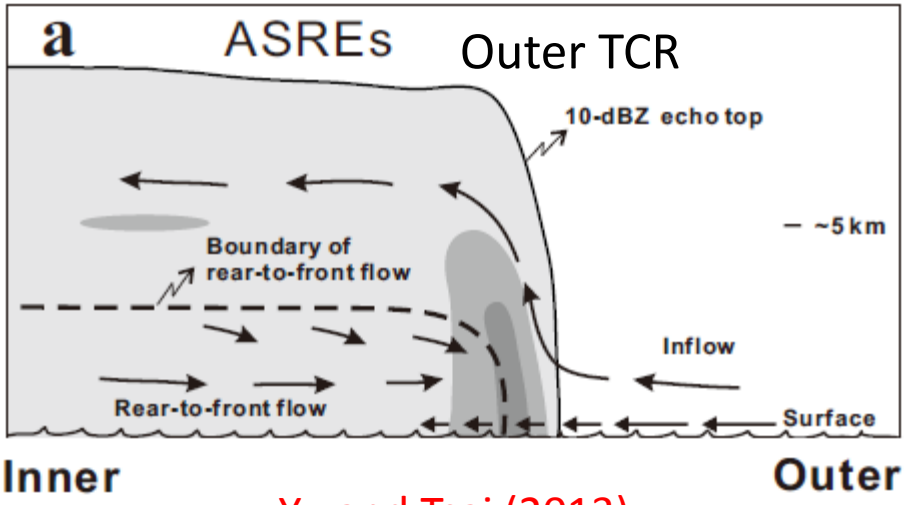

Yu and Tsai (2013)

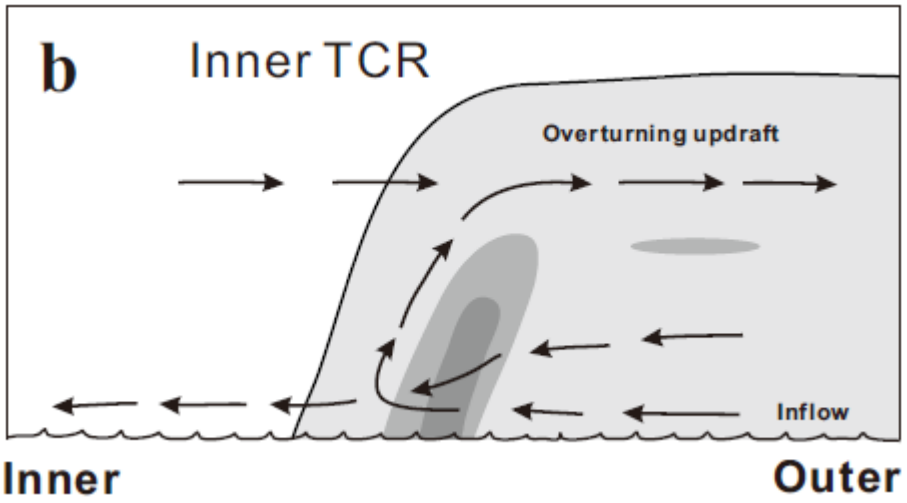

Barnes et al. (1983); Hence and Houze (2008)